Insect Biochemistry and Molecular Biology 113 (2019) 103212

Contents lists available at ScienceDirect

Insect Biochemistry and Molecular Biology

journal homepage: www.elsevier.com/locate/ibmb

A cytochrome P450 from the mustard leaf beetles hydroxylates geraniol, a key step in iridoid biosynthesis

Nanxia Fu[a], Zhi-Ling Yang[b], Yannick Pauchet[c], Christian Paetz[d], Wolfgang Brandt[e], Wilhelm Boland[a,*], Antje Burse[a,f,**]

[a] Department of Bioorganic Chemistry, Max Planck Institute for Chemical Ecology, Hans Knöll Str. 8, 07745, Jena, Germany
[b] Research Group Sequestration and Detoxification in Insects, Max Planck Institute for Chemical Ecology, Hans Knöll Str. 8, 07745, Jena, Germany
[c] Department of Entomology, Max Planck Institute for Chemical Ecology, Hans Knöll Str. 8, 07745, Jena, Germany
[d] Research Group Biosynthesis/NMR, Max Planck Institute for Chemical Ecology, Hans Knöll Str. 8, 07745, Jena, Germany
[e] Department of Bioorganic Chemistry, Leibniz Institute of Plant Biochemistry, Weinberg 3, 06120, Halle (Saale), Germany
[f] Department of Medical Technology and Biotechnology, Ernst Abbe Hochschule Jena, Carl Zeiss Promenade 2, 07745, Jena, Germany

ARTICLE INFO

Keywords:
Chrysomelidae
Chemical defense
Iridoid
P450 monooxygenase
Fat body
Phaedon cochleariae

ABSTRACT

Larvae of the leaf beetle *Phaedon cochleariae* synthesize the iridoid chysomelidial via the mevalonate pathway to repel predators. The normal terpenoid biosynthesis is integrated into the dedicated defensive pathway by the ω-hydroxylation of geraniol to (2*E*,6*E*)-2,6-dimethylocta-2,6-diene-1,8-diol (ω–OH–geraniol). Here we identify and characterize the P450 monooxygenase CYP6BH5 as the geraniol hydroxylase using integrated transcriptomics, proteomics and RNA interference (RNAi). In the fat body, 73 cytochrome P450s were identified, and *CYP6BH5* was among those that were expressed specifically in fat body. Double stranded RNA mediated knockdown of *CYP6BH5* led to a significant reduction of ω-hydroxygeraniol glucoside in the hemolymph and, later, of the chrysomelidial in the defensive secretion. Heterologously expressed CYP6BH5 converted geraniol to ω–OH–geraniol. In addition to geraniol, CYP6BH5 also catalyzes hydroxylation of other monoterpenols, such as nerol and citronellol to the corresponding α,ω-dihydroxy compounds.

1. Introduction

Iridoids comprise a large family of biologically active molecules that have so far been found in plants and insects. Structurally, they are known as *cis*-fused cyclopentan-[c]-pyrans with a hydroxyl (iridoid aglucones) or glucosyloxy moiety (iridoid glucosides) at C-1 position of the pyran ring. Besides their genuine defensive function against herbivores or insect predators, extensive studies have revealed that iridoids are also pharmaceutically valuable for the development of novel drugs and therapeutic strategies against diverse conditions including inflammation and cancers (Boros and Stermitz, 1991; Ghisalberti, 1998; Laurent et al., 2004; Tundis et al., 2008; Yamane et al., 2010). However, the often low yield of iridoids from natural resources has greatly hampered their therapeutic application (Miettinen et al., 2014). Maximizing the production of iridoids to an industrial scale using metabolic engineering offers a promising solution to their current scarcity (Alagna et al., 2016; Brown et al., 2015). To facilitate the optimization of the metabolic engineering, the identification of the genes and enzymes required for iridoids biosynthesis is essential.

Madagascar periwinkle, *Catharanthus roseus*, is a well-characterized iridoid-producing medicinal plant. Recently, all genes and enzymes involved in the iridoid biosynthetic pathway were completely elucidated in *C. roseus* (Krithika et al., 2015; Larsen et al., 2017; Miettinen et al., 2014). Although iridoids are typically encountered in the plant kingdom, they are also known from arthropods. For example, the oribatid mite, *Oribotritia berlesei* and several Coleoptera insects use iridoids as defensive compounds; the female parasitic wasp, *Leptopilina heterotoma*, and the sexual female of rosy apple aphid, *Dysaphis plantaginea*, release iridoids as mating pheromones (Cavill et al., 1984; Dinda, 2019; Oldham et al., 1996; Raspotnig et al., 2008; Smith et al., 1979). In fact, the name iridoid is a generic term derived from iridomyrmecin, iridolactone and iridodial, components of defensive secretions identified from species of the ant genus *Iridomyrmex* (Cavill et al., 1984). However, in insects, the iridoid pathway has been characterized in only a few species, and even in *Iridomyrmex*, the pathway is not yet fully resolved (Cavill et al., 1984). The best-investigated insect

* Corresponding author.
** Corresponding author. Department of Bioorganic Chemistry, Max Planck Institute for Chemical Ecology, Hans Knöll Str. 8, 07745, Jena, Germany.
E-mail addresses: Boland@ice.mpg.de (W. Boland), aburse@ice.mpg.de (A. Burse).

https://doi.org/10.1016/j.ibmb.2019.103212
Received 4 May 2019; Received in revised form 8 August 2019; Accepted 8 August 2019
Available online 16 August 2019
0965-1748/

Fig. 1. The paired defensive glands of the third instar *P. cochleariae* larva. The larva was stimulated to secrete defense droplets containing the iridoid chrysomelidial. Scale bar, ~0.5 cm.

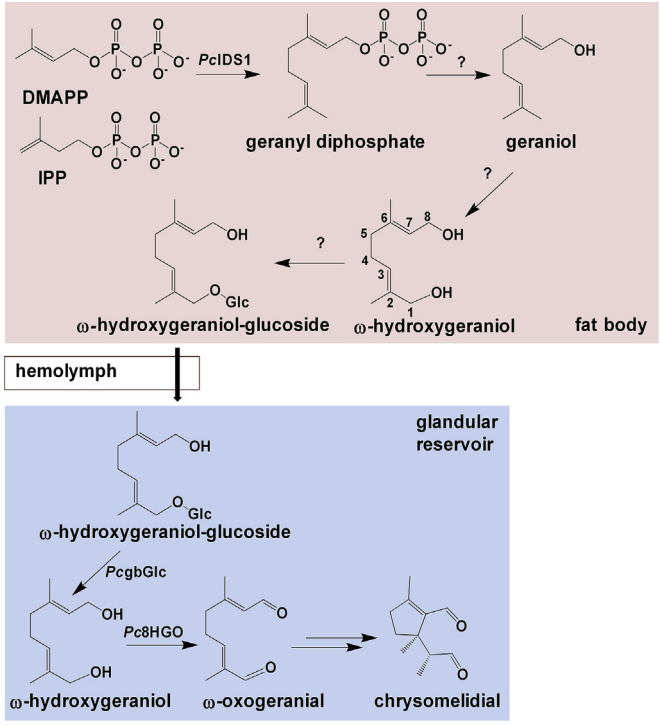

Fig. 2. Iridoid biosynthetic pathway. Adopted and modified from Burse et al. (2007).

species so far belong to the beetle family Chrysomelidae (leaf beetles). In particular, larvae of Chrysomelina beetles, such as the mustard leaf beetle, *Phaedon cochleariae*, have evolved specialized paired exocrine glands (composed of a reservoir with adhering glandular cells) to fend off predators (Fig. 1); these glands, located laterally on the dorsum of the larvae, are able to release defensive droplets containing the iridoid chrysomelidial. As shown in Fig. 2, the *de novo* biosynthesis of chrysomelidial starts in larvae of *P. cochleariae* with the formation of the early stage precursor ω-hydroxygeraniol glucoside (ω–OH–Ger-Glc) in the fat body, which is transported via the hemolymph into the glandular reservoir (Burse et al., 2009, 2007; Frick et al., 2013; Strauss et al., 2013). In the glandular reservoir, ω–OH–Ger-Glc is subject to sequential hydrolysis, oxidation and cyclization to form the ultimate product, chrysomelidial (Bodemann et al., 2012; Rahfeld et al., 2015, 2014; Strauss et al., 2013). Although most of the glandular enzymes involved in the later steps of the pathway are well characterized, to date only a few enzymes from the early biosynthetic steps have been functionally characterized (Burse et al., 2009; Frick et al., 2013; Kunert et al., 2013; Rahfeld et al., 2015; Strauss et al., 2013). Similar to other monoterpernoids, iridoid biosynthesis in *P. cochleariae* is produced from geranyl diphosphate (GDP), a compound that is synthesized along the mevalonate pathway (Frick et al., 2013; Snyder and Qi, 2013). GDP is further transformed to the shuttling glucoside ω–OH–Ger-Glc.

Stable isotope labeling studies indicated the production of the shuttling glucoside ω–OH–Ger-Glc in *P. cochleariae* was likely to proceed as follows (Oldham et al., 1996; Veith et al., 1994). First, the phosphate group is removed from GDP by a presumptive phosphatase, yielding geraniol (Cao et al., 2009; Nyati et al., 2013). Next, an oxidase converts geraniol into the diol (2*E*,6*E*)-2,6-dimethylocta-2,6-diene-1,8-diol (ω–OH–geraniol) (Veith et al., 1994). In a final step, a glucosyltransferase catalyzes the addition of a sugar moiety to form the desired shuttling glucoside (Kunert et al., 2013). In *C. roseus,* the hydroxylation from geraniol to ω–OH–geraniol is catalyzed by a cytochrome P450 (Collu et al., 2001). It is hypothesized that the enzymatic system that produces ω-OH-geraniol in *P. cochleariae* larvae may have similar characteristics as that in plants. However, the molecular characteristics of such an enzyme remain elusive.

Using an integrated approach coupling transcriptomics, proteomics and RNAi, we identified a cytochrome P450, CYP6BH5, in *P. cochleariae* larvae as the genuine geraniol 8-hydroxylase involved in chrysomelidial biosynthesis. Substrate specificity analysis demonstrated that CYP6BH5 is a promiscuous enzyme, which may serve as an alternative catalyst for the production of iridoids via metabolic engineering.

2. Materials and methods

2.1. Leaf beetles

The mustard leaf beetle, *P. cochleariae*, was reared in the lab on Chinese cabbage *Brassica oleracea* convar. *capitata* var. *alba* (Gloria F1) under 16 h light to 8 h dark cycle conditions at 15 ± 2 °C. *Chrysomela populi* (L.) were collected near Dornburg, Germany (+51°00′52.00″, +11°38′17.00″), on *Populus maximowiczii* x *Populus nigra*. The beetles were then lab-reared under 18 °C ± 2 °C in light (16 h) and 13 °C ± 2 °C in darkness (8 h) cycle conditions.

2.2. RNA extraction and cDNA synthesis

Different tissues (fat body, gut, defensive glands and Malpighian tubules) of third instar larvae of *P. cochleariae* were dissected under the microscope and stored in 100 µl lysis-buffer (Life Technologies, Carlsbad, CA, USA) with addition of 1 µl ExpressArt NucleoGuard (Amp Tec GmbH, Hamburg, Germany) at −80 °C until needed. Total RNA from stored tissues was isolated with RNAqueous®-Micro Kit (Life Technologies, Carlsbad, CA, USA) according to the manufacturer's instructions. The RNA from the larvae of *P. cochleariae* and *C. populi* was isolated with the RNAqueous kit (Life Technologies, Carlsbad, CA, USA). All RNA samples were stored at −80 °C after extraction. For RNA samples used for quantitative real-time PCR (qPCR), the genomic DNA was digested by DNase I (Thermo Fisher Scientific, Langenselbold, Germany) prior to cDNA synthesis.

For cDNA synthesis, a total of 400 ng RNA was used together with 1 µl SuperScript III Reverse Transcriptase (Life Technologies, Carlsbad, CA, USA) and 0.5 µg/µl Oligo(dT)$_{12\text{-}18}$ Primers (Life Technologies, Carlsbad, CA, USA) per 20 µl reaction. The cDNA template from the fat body of *P. cochleariae* for 3′ rapid amplification of cDNA ends (3′ RACE) was synthesized according to the manual from SMARTer RACE 5′/3′ Kit (Takara Bio, Inc. Mountain View, CA, USA). All cDNA templates were stored at −20 °C after synthesis.

2.3. Membrane proteomics and annotation of the cytochrome P450s in the fat body

To extract membrane protein, 100–200 mg fat body was used for extraction. The membrane fractions were separated and collected via ultra-centrifugation at 100,000 g. Afterwards, the membrane fractions were dissolved in 5x SDS buffer (50 mM Tris-HCl pH 6.8, 2% SDS, 10% glycerol, 1% β-mercaptoethanol, 12.5 mM EDTA, 0.02% bromophenol blue) and stored at −20 °C until needed. Proteins of the membrane fractions were separated by SDS PAGE and then stained with Coomassie blue. Proteomic analysis was performed by liquid chromatography-mass spectrometry (LC-MS^E) according to Rahfeld et al. (2015). The proteomic data were processed with our in-house *P. cochleriae* transcriptome database (Stock et al., 2013). Finally, Pfam and Blast2Go analysis were used to identify all fat body cytochrome P450s.

2.4. Analysis of the expression pattern in selected tissues

Reverse transcription-qPCR (RT-qPCR) was performed to analyze the expression pattern of selected P450 candidates in different tissues (fat body, gut, Malpighian tubules and defensive glands) with Bio-Rad CFX96 real time PCR detection system (Bio-Rad Laboratories, Munich, Germany). Each RT-qPCR reaction (20 µl final volume) contained 10 µl Brilliant III SYBR Green qPCR Master Mix (Agilent Technologies, Waldbronn, Germany), 0.6 µl of cDNA, and 0.2 µl each of forward and reverse gene-specific primers (Table S2). The initial incubation took place at 95 °C for 3 min, followed by 40 cycles at 95 °C for 10 s, 60 °C for 20 s, and at 72 °C for 30s. Three technical replicates were applied to three biological replicates. Technical replicates with a Cq difference > 0.5 were excluded. Elongation factors 1a (*Pc* EF1a) and the eukaryotic translation initiation factor 4a (*Pc* eIF4a) were chosen as reference genes for normalization. Primers were designed by primer3-plus (http://www.bioinformatics.nl/cgibin/primer3plus/primer3plus.cgi); all primer sequences can be found in Table S2. All assays were performed according to MIQE-guidelines (Bustin et al., 2009).

2.5. Knockdown of candidate genes by RNA interference (RNAi)

The assembled sequences of selected candidates were analyzed by siFi 21 (https://sourceforge.net/projects/sifi21/) for off-target prediction using a threshold value of at least 21 continuous nucleotides. The unique fragments (> 400 bp) were used to design dsRNA primers (Table S2) and all dsRNA fragments (including the ds *eGFP* control) were synthesized using the MEGAscript RNAi Kit (Thermo Fisher Scientific, Langenselbold, Germany). After purification, the dsRNA was diluted in 0.9% NaCl solution and adjusted to a concentration of 2 µg/µl. Second instar *P. cochleariae* larvae were anesthetized on ice prior to injection. For each larva, 100 ng dsRNA was injected into the haemocoel from region between the pro- and mesothorax under the microscope with a glass capillary mounted to a Nano2000 injector (WPI, Sarasota, FL, USA). Larvae injected with only dsRNA targeting *eGFP* were used as a control group. After injection, the larvae were transferred into insect rearing cups and kept under normal rearing conditions.

2.6. Collection of hemolymph and the glandular secretion

Larval glandular secretion and hemolymph were collected by glass capillaries (i.d.: 0.28 mm, o.d.: 0.78 mm, length: 100 mm; Hirschmann, Eberstadt, Germany) and then transferred to a 200 µl Eppendorf tube according to Kunert et al. (2008). The weight of the glandular secretion and hemolymph were obtained by weighing empty and filled tubes with hemolymph or secretion. Samples were stored at −20 °C until needed.

2.7. Amplification and sub-cloning of the CYP6BH5 open reading frame (ORF)

To obtain the full-length ORF, RACE-PCR was conducted with combination of fat body 3′RACE ready cDNA and RACE primers (Table S2) according to the manufacturer's protocol (Takara Bio, Mountain View, CA, USA). The ORF was obtained by assembling the RACE fragment and the corresponding fragment obtained from the transcriptome. Afterwards, the ORF sequence was re-amplified with Phusion High-Fidelity DNA Polymerase (Life Technologies, Carlsbad, CA, USA) and the corresponding primers (Table S2). The complete ORF sequence of *CYP6BH5* (accession number: MK843790) was verified by sequencing.

To produce the recombinant protein, *CYP6BH5* was sub-cloned into pcDNA™3.1D/V5-His-TOPO and pFastBac Dual expression vectors, respectively, according to the manufacturer's protocol (Thermo Fisher Scientific, Langenselbold, Germany). To facilitate detection of the recombinant proteins, constructs without a stop codon were sub-cloned in parallel into corresponding expression vectors. A *C. populi* cytochrome P450 reductase (*CPR,* accession number: MK843791) was cloned and subjected to operations similar to those procedures mentioned above. All primers for sub-cloning can be found in Table S2.

2.8. Expression of the recombinant proteins and microsome isolation

To produce recombinant proteins in HEK cells, the recombinant pcDNA™3.1D/V5-His-TOPO plasmids of *CYP6BH5* and *CPR* were co-transfected in a ratio of 4:1 into HEK cells by electroporation. HEK cells were maintained at 37 °C with 10% CO_2. After 48 h, cells were harvested and washed with phosphate-buffered saline (PBS), and the microsomal fraction was prepared as described by Joussen et al. (2012) and stored at −80 °C. To produce recombinant proteins with Sf9 cells, the bacmids were transfected into the Sf9 insect cells using a Bac-to-Bac baculovirus expression system according to the manual (Thermo Fisher Scientific, Langenselbold, Germany). The titer of the recombinant virus was determined following manufacturer's instructions. Sf9 cells were co-infected with recombinant baculoviruses expressing CYP6BH5 and CPR with a multiplicity of infection (MOI) of 1 and 0.1, respectively. Sf9 cells were maintained at 27 °C with Sf-900 II SFM medium (Life Technologies, Carlsbad, CA, USA), supplemented with 2.5 µg/ml hemin and 0.3% (vol/vol) fetal bovine serum (Atlas Biologicals, Fort Collins,CO, USA). After 72 h, cells were harvested for isolation of the microsomal fraction. The microsomal fraction was aliquoted and stored at −80 °C after protein quantification with the Quick Start Bradford Protein Assay Kit (Bio-Rad Laboratories, Munich, Germany).

2.9. SDS PAGE and Western blot

Microsomal fractions containing CYP6BH5 and CPR, fused with a V5 epitope tag and a His-tag were denatured by incubation at 70 °C for 5 min and followed by SDS PAGE separation. Afterwards, membrane proteins were blotted onto a polyvinylidene difluoride (PVDF) membrane (Trans-Blot® Turbo™ Mini PVDF Transfer Pack; Bio-Rad) with a Bio-Rad blotting system. The membrane was blocked first in blocking buffer (5% (wt/vol) non-fat dry milk in Tris-buffered saline with Tween-20 (TBST) buffer) for 1 h and then incubated overnight with Anti-V5-HRP antibody (1:10,000; Thermo Fisher Scientific, Langenselbold, Germany) in another blocking buffer (0.25% (wt/vol) non-fat dry milk in TBST buffer) at 4 °C. The membrane was washed three times with TBST buffer prior to incubation (1 min) with enhanced chemiluminescence (ECL) solution (Thermo Fisher Scientific, Langenselbold, Germany). The Amersham Hyperfilm ECL X-ray film (GE Healthcare, Boston, USA) was exposed to the PVDF membrane prior to developing the film.

2.10. Enzyme assays

The microsomal fraction with the recombinant proteins lacking the V5 epitope and His-tag was used for the enzyme assay. The assay was performed in 50 µl volume containing 25 µg microsomal proteins in 20 mM potassium phosphate buffer (pH 7.5), 200 µM substrate and 1 mM NADPH. The same assay without NADPH served as the negative control. The empty control, in contrast, contained 25 µg microsomal proteins obtained from cells that were infected with only the recombinant CPR virus. After incubation at 30 °C for 15 min, the reaction was stopped and extracted by the addition of an equal volume of ethyl acetate. Samples were silylated by *N*-methyl-*N*-(trimethylsilyl) trifluoroacetamide (MSTFA) prior to gas chromatography-mass spectrometry (GC-MS) analysis.

To generate products for nuclear magnetic resonance (NMR) analysis, the standard enzyme assay was scaled up to a volume of 500 µl containing 1 mM of substrate (nerol or citronellol). After a first round of incubation with 70 µg microsomes for 1 h at 30 °C, a second aliquot of 70 µg microsomes was added and incubated for another 1 h, and those steps were repeated 5 times. The reaction was then stopped by adding 200 µl of 1 M HCl, vortexing, and cooling on ice. Two up-scaled assays for each substrate were pooled. To extract the products, equal volumes of ethyl acetate were added and the supernatants were collected. The solvent of the samples was removed by a stream of nitrogen gas.

2.11. GC-MS, high performance liquid chromatography-mass spectrometry (HPLC-MS) and NMR analysis

To detect chrysomelidial, the stored larval secretion was dissolved in 25 µl ethyl acetate spiked with 2 µg/µl methyl benzoate, and the supernatant was transferred to GC vials. One microliter was subjected to GC-MS analysis [ThermoQuest ISQ mass spectrometer EI LI system (quadrupole) equipped with Phenomenex ZB-5-W/Guard Column, 25 m (10 m Guard Pre-column) × 0.25 mm, film thickness of 0.25 µm]. The program setting was the same as previously reported (Rahfeld et al., 2014). The peak areas were calculated by Thermo Xcalibur Quan Brower that is implemented in the Xcalibur software (Thermo Fisher Scientific, Langenselbold, Germany). The relative amount of chrysomelidial per µg secretion was calculated against the amount of methyl benzoate spiked in the solvent.

To detect the ω–OH–Ger-Glc, the stored larval hemolymph was extracted with 50 µl methanol containing 0.025 mM ω-hydroxygeraniol-thio-β-D-glucoside (ω–OH–Ger-S-Glc). The supernatant was collected and subjected to HPLC–MS analysis. Condition for the measurement and identification of ω–OH–Ger-Glc and ω–OH–Ger-S-Glc followed the method optimized by Kunert et al. (2008). The peak areas were calculated as mentioned earlier. The relative amount of ω–OH–Ger-Glc per µg hemolymph was calculated against the internal standard ω–OH–Ger-S-Glc.

For the detection of ω–OH–geraniol by GC-MS in extracts and enzyme assays, the hydroxyl groups of the analytes were first silylated with MSTFA at 70 °C for 30 min. Then, the sample was dried under nitrogen and re-suspended in ethyl acetate. One microliter was used for GC-MS analysis under programmed conditions: 50 °C (2 min), 10 °C/min to 280 °C, 30 °C/min to 310 °C (1 min). The inlet temperature was 230 °C and the transfer line was kept at 280 °C. ω–OH–geraniol was identified by comparing the retention time and mass spectra with an authentic standard. The structure of ω-hydroxynerol and ω-hydroxycitronellol was determined by NMR. ^{1}H, ^{1}H–^{1}H COSY, ^{1}H–^{13}C HSQC, ^{1}H–^{13}C HMBC and ^{1}H–^{1}H ROESY were acquired on a 700 MHz Avance III HD spectrometer equipped with a 1.7 mm cryoprobe (Bruker Biospin, Germany). Data acquisition and processing were accomplished using TopSpin ver. 3.2 (Bruker Biospin, Rheinstetten, Germany). Samples were measured in $CDCl_3$ at 293 K.

2.12. Homology modeling

The 3D-protein structure homology modeling of CYP6BH5 was performed with YASARA Version 17.12.24 (Krieger et al., 2009; Krieger and Vriend, 2014). After searching for templates in the protein database, ten appropriate X-ray templates were found (PDB-codes: 5VCC, 5VEU, 6C93, 5XA3, 6C94, 1ZOA, 3MDM, 5B2X, 2FDV) (Berman, 2000). A homology-modeling template was generated for each of these 10 X-ray templates based on alternative sequence alignment to 78 models. The quality of all homology models was evaluated using PROCHECK and ProSA II (Laskowski et al., 1993; Sippl, 1993, 1990). The model based on the X-ray structure of 5VCC (human CYP3A4), scored −1.613, and was the best, with a sequence identity of 34.2% and a sequence similarity of 55.0% (BLOSUM62 score is > 0) (Sevrioukova, 2017). This model was subsequently refined with the md-refinement tool of YASARA (20 simulated annealing runs for 500 ps). A model with excellent quality resulted, based on the Ramachandran plot: 91.5% residues were found in the most favored region, and two outliers were found only in the loop regions; all the ProSA energy graphs are in the negative range, and the calculated z-scores are in the range of natively folded proteins.

100 docking positions of geraniol were generated by docking geraniol at the active site close to the heme center using MOE 2018.01 (https://www.chemcomp.com/). Out of several alternative docking positions, the fourth one was selected because of the proximity between the C_{10}-methyl group of geraniol and the peroxide bound to heme. To confirm the stability of the arrangement, a second md-refinement run was performed.

3. Results

3.1. Presence of ω–OH–geraniol in the fat body of P. cochleariae

The aglycone ω–OH–geraniol is the first metabolite that links classical terpenoid biosynthesis to the dedicated defense metabolism. Although the presence of ω–OH–Ger-Glc in fat body extracts from *P. cochleariae* has been reported by Burse et al. (2007), the presence of the corresponding aglycone in the fat body has not been validated. Therefore, the presence of ω–OH–geraniol in this tissue was checked. As shown in Fig. 3, the production of ω–OH–geraniol in the fat body was confirmed using authentic standards (mass spectra, see Fig. S1). Moreover, its glucoside could also be detected in the fat body with HPLC-MS (Fig. S2). These observations support the hypothesis that the early biosynthetic steps of the iridoid biosynthesis pathway are localized in the fat body (Burse et al., 2007), which therefore should contain the corresponding enzymes including the geraniol oxidase and the glycosyltransferase.

3.2. Identification of P450 candidates from the P. cochleariae fat body

In order to identify the oxidase(s) involved in iridoid biosynthesis, approximately 193 transcripts (supplementary file 1) were annotated as putative cytochrome P450s in our in-house *P. cochleariae* transcriptomic reference library (Stock et al., 2013). To narrow down the number of potential P450 candidates, the sequence information was combined with the proteomic analysis of the fat body membrane proteins. A total of 73 cytochrome P450s enzymes were identified in the fat body, among them, 44 CYP6s, 12 CYP4s, 9 CYP9s, 5 CYP347s, and 1 each of CYP345, CYP349 and CYP306 (Fig. S3 and Table S1). Since the geraniol ω-hydroxylase was supposed to be a relatively abundant protein in the fat body, the matched peptide numbers of these candidates were also compared (Table S1). We selected 12 candidates that had more than 20 matched peptides for further analysis.

The expression pattern of selected candidates was an additional criterion for identifying the prominent P450 members in *P. cochleariae* fat body. RT-qPCR was carried out to measure the relative abundance of

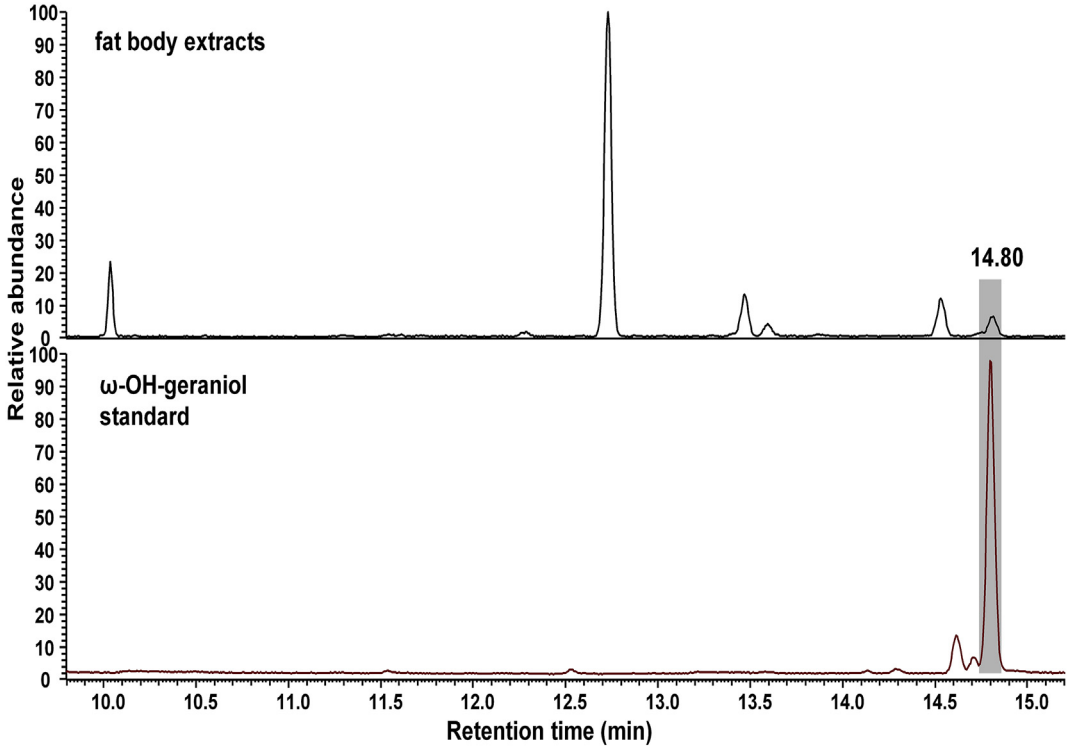

Fig. 3. Total ion current chromatograms of MSTFA silylated ω–OH–geraniol (RT: 14.80 min) in the fat body of *P. cochleariae* detected by GC-MS. ω–OH–geraniol in fat body extracts was assigned based on comparison of the retention time and mass spectra to the authentic standard. For mass spectra of the silylated ω–OH–geraniol, see Fig. S1.

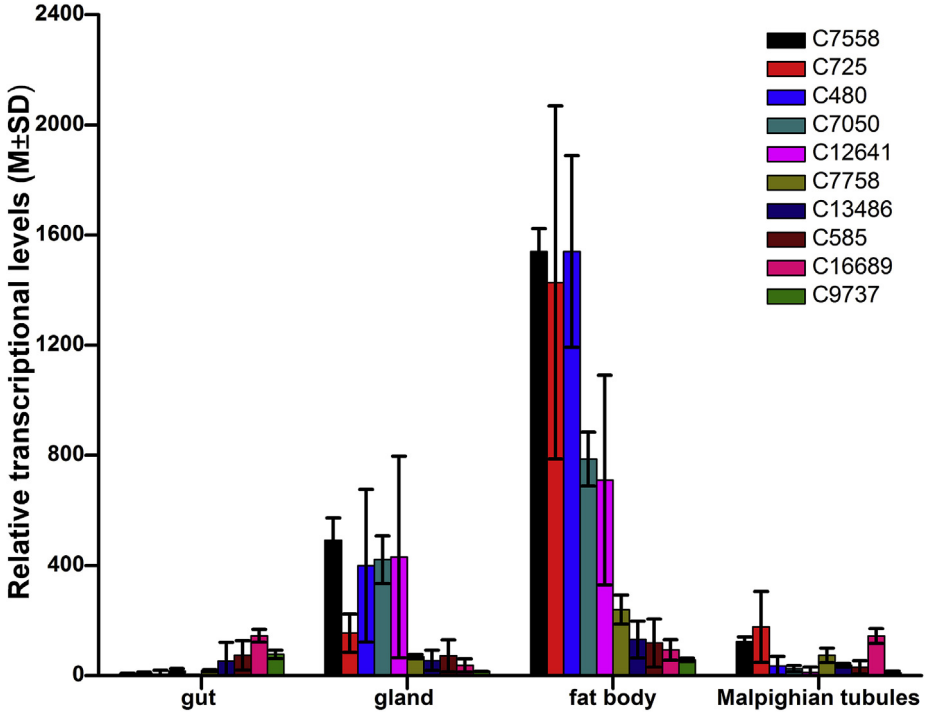

Fig. 4. The tissue specific expression profile of the selected P450 candidates in the third instar *P. cochleariae* larvae. The graph was plotted based on the values ($2^{-\Delta Cq}$) measured by RT-qPCR (n = 3).

the selected P450s from different larval tissues, including gut, Malpighian tubules, fat body and defensive glands. Since C7558, C7614 and C28218 differed from each other by only 1 or 2 amino acids, *C7558* was taken as a representative gene for RT-qPCR analysis. As shown in Fig. 4, 9 genes were more abundantly expressed in the fat body than in the other tissues. *C16689* showed higher expression levels in the gut and Malpighian tubules. Thus, these 9 P450s were considered as candidates for further analysis.

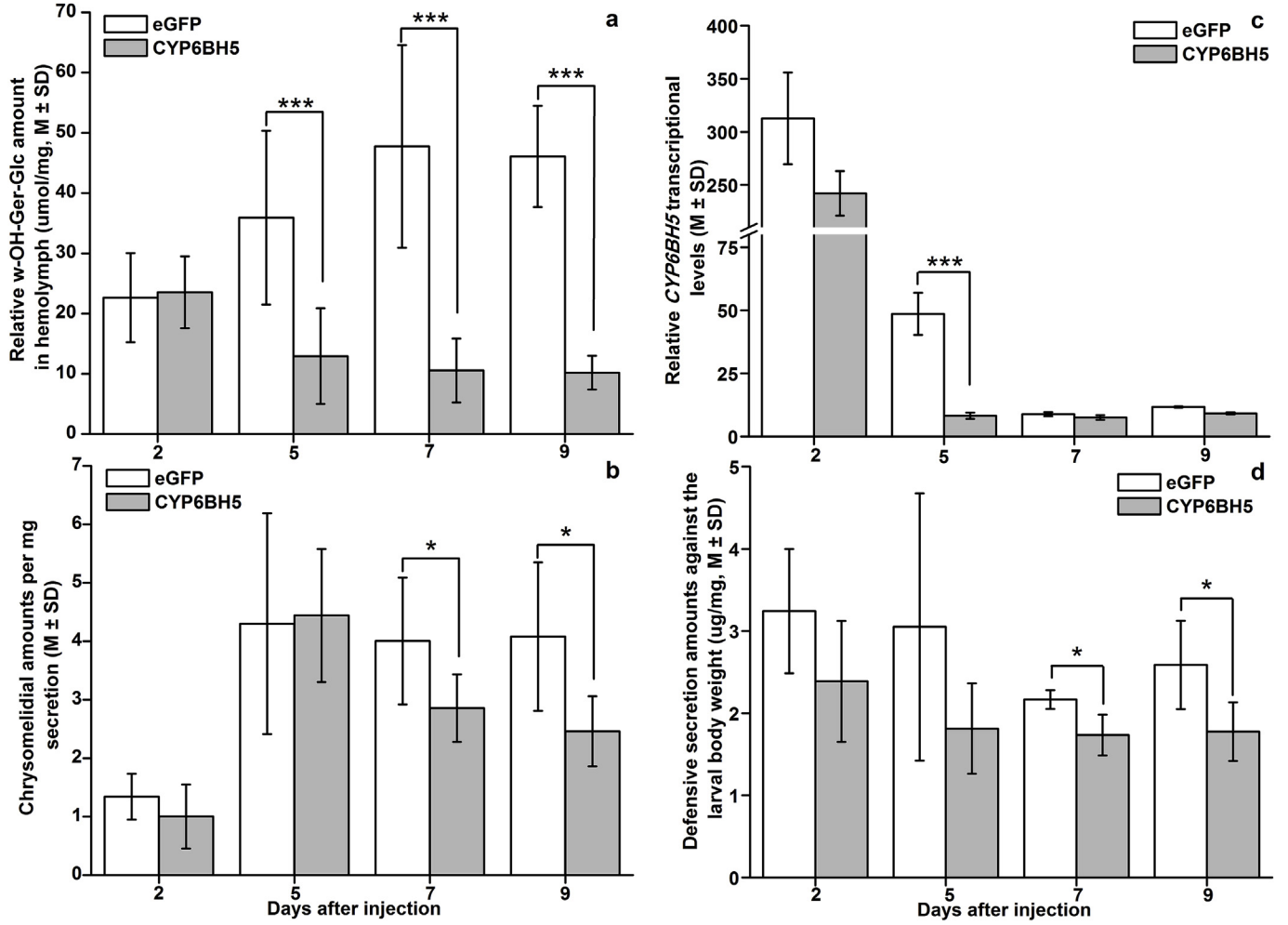

Fig. 5. Timeline of different RNAi effects. a) Relative ω-hydroxygeraniol glucoside (ω–OH–Ger-Glc) amount in the hemolymph after RNAi (n ≥ 9); b) Transcriptional level ($2^{-\Delta Cq}$) of CYP6BH5 (n = 3); c) The chrysomelidial amount in the defensive glandular secretion (n ≥ 5); d) Defensive secretion produced by larvae from CYP6BH5 and eGFP knockdown groups (n ≥ 5). The data were normalized by taking the square root before statistical analysis to pass the normality test (Shapiroe Wilk); two-tailed student's *t*-test for equal variances was used to value significance levels. Asterisks represent significant differences in CYP6BH5 knockdown larvae compared to eGFP injected control larvae (*p < 0.05, ***p < 0.001).

3.3. RNAi-based identification of P450(s) involved in iridoid biosynthesis

According to the transcripts abundance, dsRNA of the most prominent candidates was synthesized and used for silencing to identify the right candidate(s) for the iridoid biosynthesis. Second instar *P. cochleariae* larvae were used for injection, and larvae treated with dsRNA targeting *eGFP* were taken as the control group. The amount of the downstream product ω–OH–Ger-Glc present in larval hemolymph was examined via HPLC-MS. Among the 6 tested candidates, only the knockdown of *C7758* led to a significant decrease of ω–OH–Ger-Glc compared to the level in the eGFP control (Fig. S4). We further verified the observed effect of the knockdown of *C7758* by a time course sampling. As indicated in Fig. 5a, in the eGFP group the relative ω–OH–Ger-Glc amount increased gradually from 2 to 7 days after injection and then remained at a stable level. In contrast, the ds*C7758* injected group showed a significant decrease on the fifth day after injection; afterwards the compound remained at a basal low level until the larvae reached the pre-pupal stage.

The observed decrease of ω–OH–Ger-Glc from down-regulation of *C7758* was correlated with transcription analysis and larval physiological development. As shown in Fig. 5b, the relative transcription level of *C7758* in both groups showed identical and high expression upon injection. However, on the fifth day after injection, the transcriptional level in *C7758* knockdown group dropped to 2.8% of that in the eGFP control group, indicating that the RNAi effect had been triggered and the gene had been successfully knocked down. The observed low transcription level of *C7758* in the eGFP control from the seventh day on is likely due to the physiological down-regulation, as the larvae have reached the pre-pupal state, which is closely related to the non-chrysomelidial-containing pupal stage (Pasteels et al., 1988). Moreover, knocking down the expression of the *C7758* gene did not affect larval physiological development, as indicated by the similar body weight observed in the two experimental groups (Fig. S5).

In addition, we examined the knockdown effect of *C7758* on the larvae's ability to produce defensive secretion. As shown in Fig. 5c, the chrysomelidial concentration in the glandular secretion increased along with the body weight until it rose to a stable level that is characteristic for earlier stage larvae. Although, the chrysomelidial concentration in the C7758 knockdown group reached highest level on the fifth day after injection, it decreased steadily and significantly afterwards due to the lack of *C7758* transcripts. Fig. 5d indicated that the larvae tended to maintain a relatively stable level of glandular secretion despite the continuous body weight gain during the experimental period. However, the relative level in the *C7758* knockdown group was always lower, and the difference became significant from seventh days after injection. Based on our results, we concluded that *P. cochleariae* recruited the cytochrome P450 *C7758* for iridoid biosynthesis. According to the P450 nomenclature committee, this sequence is referred to as CYP6BH5.

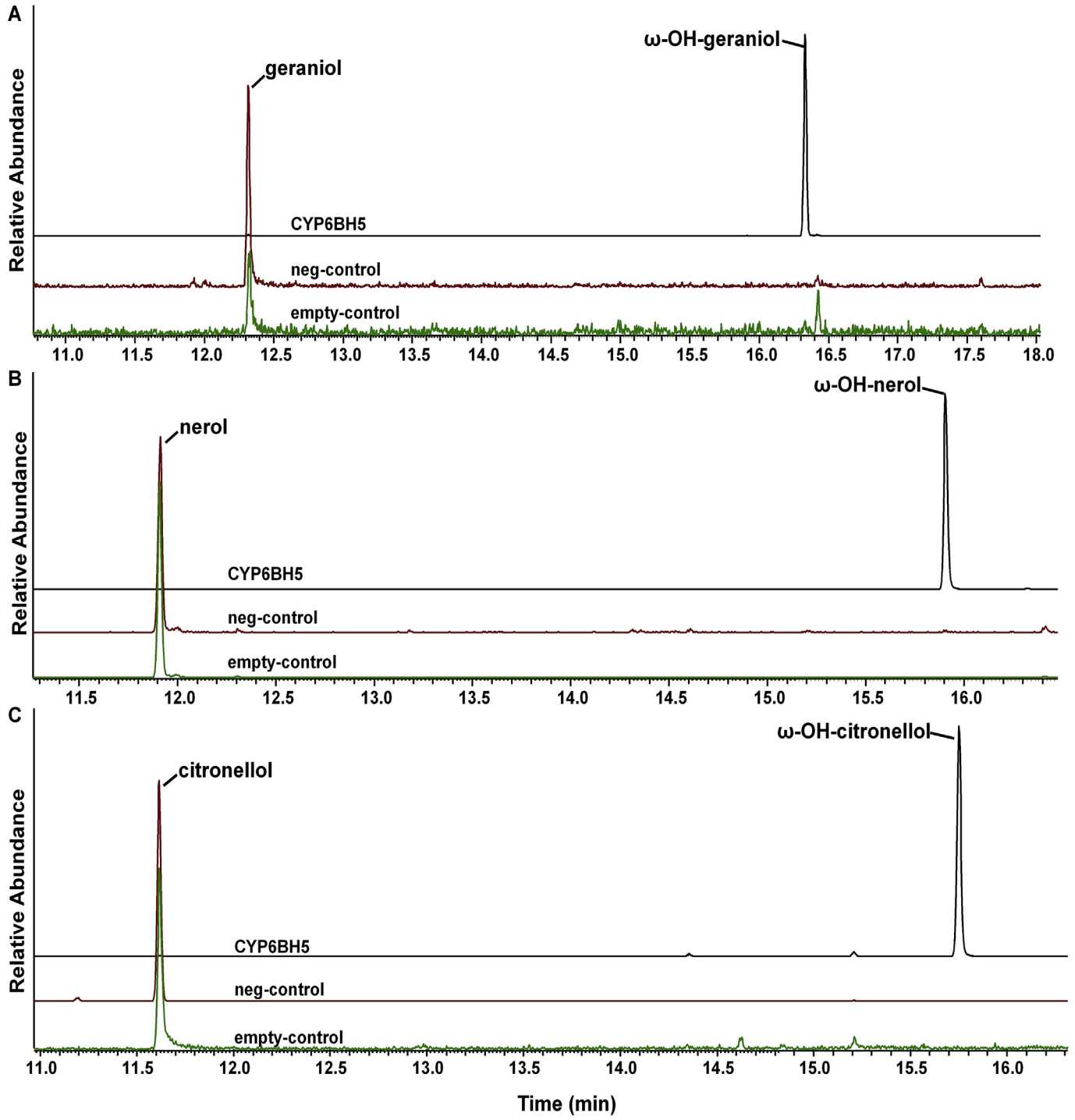

Fig. 6. GC-MS chromatograms of the reaction products show the conversion of monoterpenols by the CYP6BH5 enzyme expressed by Sf9 insect cells. The chromatograms for enzyme assays with geraniol, nerol and citronellol as substrate were extracted based on preselected m/z values at 156, 156 and 95, respectively. Microsomal fractions from Sf9 insect cells expressing CYP6BH5 and CPR or CPR only (empty-control) were incubated with 200 μM of substrate for 15 min in the presence of NADPH. No NADPH was added to the negative control (neg-control). Identified compounds were then assigned based on their retention times and mass spectra. Mass spectra and NMR data of the products and the references are available in supplementary Figures S1 and S5 to S9.

3.4. In vitro evidence of geraniol hydroxylase activity of CYP6BH5 and its substrate selectivity

Direct evidence of CYP6BH5's function as a geraniol hydroxylase was obtained *in vitro* by the functional co-expression of CYP6BH5 and CPR derived from *C. populi*. A pilot experiment with the microsomal fraction from HEK 293 cells expressing CYP6BH5 and CPR showed the transformation of geraniol to ω–OH–geraniol (Fig. S6). Due to the low yield of the recombinant proteins in HEK 293 cells, we produced CYP6BH5 and CPR in Sf9 insect cells via transient baculovirus-mediated expression (Fig. S7). Enzyme assays with recombinant CYP6BH5/CPR microsomes derived from Sf9 insect cells also revealed the conversion of geraniol into ω–OH–geraniol in the presence of NADPH. The stereochemistry was confirmed by comparison with an authentic standard. There was no detectable turnover of the substrate in either the negative-control reaction (without NADPH) or the empty control reaction

(microsome containing only CPR), see Fig. 6A (mass spectra, see Fig. S1). Because members from the CYP76 family (such as CYP76B6) were recently reported as versatile monoterpenol oxidases (Boachon et al., 2015; Hofer et al., 2014), a set of monoterpenols that are structurally related to geraniol, namely nerol, linalool, citronellol and citronellal were additionally tested. No conversion was detected when linalool or citronellal were used as substrates. By contrast, the hydroxylation of nerol and citronellol by CYP6BH5 was observed. NMR data verified that nerol was converted to (2*E*,6*Z*)-2,6-dimethylnona-2,6-dien-1-ol (ω–OH–nerol), see Fig. 6B (For mass spectra and NMR data, see Figs. S8 and S10a). Similarly, citronellol was metabolized to (*E*)-2,6-dimethyloct-2-ene-1,8-diol (ω–OH–citronellol), see Fig. 6C (For mass spectra and NMR data, see Figs. S9 and S10b). In all cases, the hydroxylation of the terpenol occurred selectively at the *trans* methyl group of the substrate. Characteristic NOE correlations (see Fig. S10) proved the assignments. Sung et al. (2011) showed CYP76B6 from *C. roseus* also plays a role in phenylpropanoid biosynthesis, catalyzing 3-hydroxylation of naringenin to produce eriodictyol. Therefore, we also tested CYP6BH5's activity on naringenin, but no reaction was noticed.

3.5. Homology modeling of CYP6BH5 with the substrate geraniol

To reveal the underlying mechanism of CYP6BH5's substrate preference for geraniol (1-ol) over linalool (3-ol), the docking of geraniol to a homology-based 3D-structure of CYP6BH5 was conducted. As shown in Fig. 7, geraniol is positioned close to the hydroperoxyl heme of the enzyme's active site. Thr303 maintains a hydrogen bridge to the distal oxygen in the ferric hydroperoxy complex and might be relevant for activation (Sezutsu et al., 2013). The docking pose is stabilized by the formation of hydrogen bonds between the hydroxyl group of geraniol and the side chain of Arg105, with the carboxyl group of the heme prosthetic group, and with the hydroxy group of Thr369. The hydrophobic side chain of Val365 also helps to stabilize the correct position by hydrophobic interactions with the prenyl moiety of geraniol. The transoid methyl group of geraniol has a distance of 3.2 Å, compared to 3.4 Å of the cisoid methyl group to the distal oxygen atom sitting in the middle of the heme center; this explained why CYP6BH5 preferentially leads to the oxidation of the *trans* methyl group of the substrate. Since the substrate geraniol was positioned by a hydrogen bond between its 1-OH group and Arg105, it is reasonable to assume that the embedding of citronellol and nerol into the active center of CYP6BH5 is controlled by the same forces leading to ω-hydroxylation at their *trans*-methyl groups. The 3-OH group of linalool led to a positioning with the terminal methyl groups away from the active site, and, hence this compound was not oxidized.

4. Discussion

The cytochrome P450s comprise a superfamily of heme-containing monooxygenases that are known to metabolize a broad range of endogenous substrates as well as xenobiotics in all living organisms (Greule et al., 2018; Manikandan and Nagini, 2018). The abundance of P450s in insects varies greatly from species to species. For example, only 44 putatively functional cytochrome P450s were found in the bumblebee *Bombus impatiens* genome, while in the genome of *Culex quinquefasciatus* mosquitoes, a total of 204 P450s was reported (Sadd et al., 2015; Yang and Liu, 2011). In this study, we identified 73 P450s in the fat body of *P. cochleariae* larvae by a combination of proteomic and transcriptomic analysis. Based on *in vivo* and *in vitro* assays, our data convincingly proved that the *P. cochleariae* CYP6BH5 is an essential enzyme for the production of the defensive monoterpenoid chrysomelidial, by converting geraniol to ω–OH–geraniol.

Thermodynamically, ω-hydroxylation of hydrocarbon chains is inherently disfavored due to the strong C–H bond strength of a terminal methyl group (Johnston et al., 2011). Homology modeling of CYP6BH5 and geraniol showed that CYP6BH5's regiospecificity is tightly controlled by the interaction of the –OH group of geraniol with CYP6BH5's catalytic pocket. The resulting steric barriers make the access of CYP6BH5's heme center to any part of the hydrocarbon chain other than the ω-carbon difficult or impossible. In addition to geraniol, *in vitro* enzyme assays showed that CYP6BH5 transforms also other monoterpenoids, such as nerol and citronellol, but not citronellal and linalool. Since CYP6BH5 failed to react with citronellal and linalool, this supported the importance of the –OH group of the substrate for coordination with the enzyme's catalytic cavity. Unlike geraniol, citronellal does not have a primary hydroxyl group and hence, no strong hydrogen bridge to Arg105 and Thr369 can be formed. In case of linalool with a tertiary hydroxyl group at C3, the prenyl moiety does not come close enough to the heme center of CYP6BH5 to become hydroxylated. However, Boachon et al. (2015) showed that *P. cochleariae* could feed on linalool-releasing *Arabidopsis* as well as on cabbage leaves treated with pure linalool. Hence, it is postulated that *P. cochleariae* harbors a presumable P450 that differs from the geraniol 8-hydroxylase CYP6BH5 for linalool metabolism.

The monoterpenoid geraniol is known as a constituent of essential oils from more than 160 plant species, especially the *Cymbopogon* genus (Burdock, 2016). Studies showed geraniol exhibits insecticidal and repellent properties to arthropods such as mosquitoes and cockroaches, or to nematodes, ticks, etc. (Chen and Viljoen, 2010; Nasiou and Giannakou, 2018). Therefore, it is hypothesized that other insects may have also enzymes to detoxify geraniol. Until now, CYP6BH5 is the first

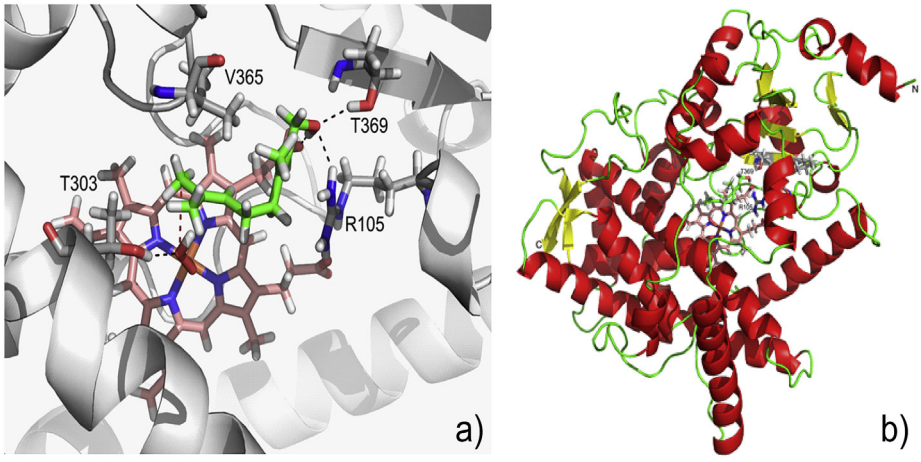

Fig. 7. Docking arrangement of geraniol in the active site of CYP6BH5. a) The hydroxyl group of geraniol is recognized by hydrogen bonds with Thr369 and Arg105 as well as by the carboxyl moiety of heme. Furthermore, the side chain of Val365 supports the correct positioning by hydrophobic interactions with the prenyl moiety. The transoid methyl group has a distance of 3.2 Å and the cisoid methyl group of 3.4 Å to the distal oxygen atom sitting in the middle of the heme center. Therefore, the enzyme will preferentially lead to oxidation of the trans methyl group. The conserved Thr303 of CYP6BH5 might be relevant for activation. Oxygen is red, carbon is green, nitrogen is blue, hydrogen is white and iron is brown. b) Tertiary structure of CYP6BH5 with bound geraniol (green carbon atom) located above the heme in the center of the enzyme (orange carbon atoms). As shown in a) the hydroxyl group of geraniol is nicely recognized by Arg105 located at the beginning of a short α-helix close to the N-terminus and by Thr369 from an anti-parallel ß-sheet. (For interpretation of the references to colour in this figure legend, the reader is referred to the Web version of this article.)

identified insect P450 that catalyzes the ω-hydroxylation of geraniol and its structurally related monoterpene alcohols, nerol and citronellol. A similar sesquiterpenoid ω-hydroxylase, namely the CYP4C7 from the cockroach *Diploptera punctata*, was reported to accept (2*E*,6*E*)-farnesol and juvenile hormone III as substrates (Sutherland et al., 1998). Apart from ω-hydroxylation, backbone hydroxylation and epoxidation are other common reactions that certain insect P450s use to transform terpenols. For example, the bark beetle *Ips pini* recruit members from CYP9T subfamily to hydroxylate the monoterpene myrcene to ipsdienol to produce aggregation pheromones (Sandstrom et al., 2008, 2006; Song et al., 2013). CYP15A1 from *D. punctata*, CYP6A1 from *Musca domestica* and CYP345E2 from *Dendroctonus ponderosae* were shown to epoxidize a variety of terpenes or terpenoids (Andersen et al., 1997; Helvig et al., 2004; Keeling et al., 2013). To uncover the relevant determinants of the regio- and stereo-selectivities of terpene oxidations observed in different insect P450s, the elucidations of the corresponding enzyme structures are essential.

In plants, members from the CYP76C subfamily and other CYP76s are used for monoterpenol oxidation (Collu et al., 2001; Hofer et al., 2013). However, compared to these plant-derived P450s, CYP6BH5 showed a narrower substrate spectrum, as indicated by the absence of detectable activity on linalool and citronellal. This feature reveals that *P. cochleariae* may have recruited CYP6BH5 specifically for the hydroxylation of large amounts of geraniol for the iridoid biosynthesis. In spite of that, CYP6BH5, like other members from CYP76s, is a substrate-promiscuous enzyme with regard to its activity on monoterpenols (Hofer et al., 2013, 2014). The observed substrate spectrum similarity among P450 enzymes that are not closely related suggests that the insects and plants obtain the geraniol 8-hydroxylases eventually via convergent evolution.

Apart from *P. cochleariae*, the Madagascar periwinkle (*C. roseus*) also uses geraniol as precursor for iridoid biosynthesis (Miettinen et al., 2014). In this plant, the iridoid (nepetalactol) serves as a precursor for secologanin, which can be metabolized further into pharmacologically important monoterpene indole alkaloids, such as vinblastine and vincristine (Alagna et al., 2016; Caputi et al., 2018; Kellner et al., 2015; Miettinen et al., 2014). In both organisms, the biosynthesis from geraniol to the iridoid shares a similar sequence and individual steps, although the enzymes are not identical. Though both organisms recruited a member from the cytochrome P450 superfamily to generate ω–OH–geraniol, the geraniol 8-hydroxylase CYP6BH5 from *P. cochleariae* shares only 20% amino acid identity to CYP76B6 in *C. roseus*. Afterwards, *P. cochleariae* uses a 8-hydroxygeraniol oxidase (*Pc* 8HGO) from the GMC oxidoreductase superfamily to produce 8-oxogeranial, whereas *C. roseus* takes either the CYP76B6 or a NAD^+ -dependent 8-hydroxygeraniol oxidoreductase belonging to the medium-chain reductase superfamily (Hofer et al., 2013; Miettinen et al., 2014; Rahfeld et al., 2014). For the ring closure, a member of the Rossmann-fold NAD $(P)^+$-binding protein superfamily, namely, the iridoid synthase is used to cyclize the 8-oxogeranial in *C. roseus* (Geu-Flores et al., 2012). In *P. cochleariae*, although knocking down a member of the juvenile hormone-binding protein superfamily led to the accumulation of the precursor 8-oxogeranial in glandular secretion, the heterologously expressed protein failed to cyclize 8-oxogeranial to chrysomelidial (Bodemann et al., 2012).

The elucidation of the enzymes involved in the iridoid biosynthetic pathway in both *P. cochleariae* and *C. roseus* lays the foundation for producing pharmacologically valuable monoterpenoid indole alkaloids on an industrial level. Recently, attempts to reconstruct the biosynthetic pathways for nepetalactol, vindoline and strictosidine from the geranyl diphosphate in yeast *Saccharomyces cerevisiae* have made impressive progress (Billingsley et al., 2017; Brown et al., 2015; Campbell et al., 2016; Qu et al., 2015). Despite the effort to use genetic engineering to optimize the performance of the platform strains, the ω-hydroxylation of geraniol at C-8 remains a bottleneck (Brown et al., 2015). The newly identified CYP6BH5 from *P. cochleariae* may serve as an alternative biocatalyst for overcoming this obstacle, further boosting the yields of monoterpenoid indole alkaloids.

Declarations of interest

None.

Acknowledgments

We sincerely thank Dr. Maritta Kunert for her support in chemical analysis, Dr. Ding Wang and Lydia Schmidt for their help with bioinformatics, Prof. Stefan H. Heinemann for his help with HEK cells, and Dr. Nicole Joußen for her constructive suggestions about P450 enzymes. The authors would also like to express their gratitude to Sarah Baur for her help in constructing the plasmids, to David Nelson (University of Tennessee) for help with P450 nomenclature and to Emily Wheeler for her critical reading of the manuscript. This work was financially supported by the Max Planck Society and the China Scholarship Council [grant number 201406300098].

Appendix A. Supplementary data

Supplementary data to this article can be found online at https://doi.org/10.1016/j.ibmb.2019.103212.

References

Alagna, F., Geu-Flores, F., Kries, H., Panara, F., Baldoni, L., O'Connor, S.E., Osbourn, A., 2016. Identification and characterization of the iridoid synthase involved in oleuropein biosynthesis in olive (olea europaea) fruits. J. Biol. Chem. 291, 5542–5554. https://doi.org/10.1074/jbc.M115.701276.

Andersen, J.F., Walding, J.K., Evans, P.H., Bowers, W.S., Feyereisen, R., 1997. Substrate specificity for the epoxidation of terpenoids and active site topology of house fly cytochrome P450 6A1. Chem. Res. Toxicol. 10, 156–164. https://doi.org/10.1021/tx9601162.

Berman, H.M., 2000. The protein data bank. Nucleic Acids Res. 28, 235–242. https://doi.org/10.1093/nar/28.1.235.

Billingsley, J.M., DeNicola, A.B., Barber, J.S., Tang, M.-C., Horecka, J., Chu, A., Garg, N.K., Tang, Y., 2017. Engineering the biocatalytic selectivity of iridoid production in Saccharomyces cerevisiae. Metab. Eng. 44, 117–125. https://doi.org/10.1016/j.ymben.2017.09.006.

Boachon, B., Junker, R.R., Miesch, L., Bassard, J.-E., Höfer, R., Caillieaudeaux, R., Seidel, D.E., Lesot, A., Heinrich, C., Ginglinger, J.-F., Allouche, L., Vincent, B., Wahyuni, D.S.C., Paetz, C., Beran, F., Miesch, M., Schneider, B., Leiss, K., Werck-Reichhart, D., 2015. CYP76C1 (cytochrome P450)-mediated linalool metabolism and the formation of volatile and soluble linalool oxides in Arabidopsis flowers: a strategy for defense against floral antagonists. Plant Cell 27, 2972–2990. https://doi.org/10.1105/tpc.15.00399.

Bodemann, R.R., Rahfeld, P., Stock, M., Kunert, M., Wielsch, N., Groth, M., Frick, S., Boland, W., Burse, A., 2012. Precise RNAi-mediated silencing of metabolically active proteins in the defence secretions of juvenile leaf beetles. Proc. R. Soc. Biol. Sci. 279, 4126–4134. https://doi.org/10.1098/rspb.2012.1342.

Boros, C.A., Stermitz, F.R., 1991. Iridoids. An updated review, Part II. J. Nat. Prod. 54, 1173–1246. https://doi.org/10.1021/np50077a001.

Brown, S., Clastre, M., Courdavault, V., O'Connor, S.E., 2015. De novo production of the plant-derived alkaloid strictosidine in yeast. Proc. Natl. Acad. Sci. U. S. A. 112, 3205–3210. https://doi.org/10.1073/pnas.1423555112.

Burdock, G.A., 2016. Fenaroli's Handbook of Flavor Ingredients, sixth ed. CRC Press, Boca Raton. https://doi.org/10.1201/9781439847503.

Burse, A., Frick, S., Discher, S., Tolzin-Banasch, K., Kirsch, R., Strauss, A., Kunert, M., Boland, W., 2009. Always being well prepared for defense: the production of deterrents by juvenile Chrysomelina beetles (Chrysomelidae). Phytochemistry 70, 1899–1909. https://doi.org/10.1016/j.phytochem.2009.08.002.

Burse, A., Schmidt, A., Frick, S., Kuhn, J., Gershenzon, J., Boland, W., 2007. Iridoid biosynthesis in Chrysomelina larvae: fat body produces early terpenoid precursors. Insect Biochem. Mol. Biol. 37, 255–265. https://doi.org/10.1016/j.ibmb.2006.11.011.

Bustin, S.A., Benes, V., Garson, J.A., Hellemans, J., Huggett, J., Kubista, M., Mueller, R., Nolan, T., Pfaffl, M.W., Shipley, G.L., Vandesompele, J., Wittwer, C.T., 2009. The MIQE guidelines: minimum information for publication of quantitative real-time PCR experiments. Clin. Chem. 55, 611–622. https://doi.org/10.1373/clinchem.2008.112797.

Campbell, A., Bauchart, P., Gold, N.D., Zhu, Y., De Luca, V., Martin, V.J., 2016. Engineering of a nepetalactol-producing platform strain of Saccharomyces cerevisiae for the production of plant seco-iridoids. ACS Synth. Biol. 5, 405–414. https://doi.org/10.1021/acssynbio.5b00289.

Cao, L., Zhang, P., Grant, D.F., 2009. An insect farnesyl phosphatase homologous to the N-

terminal domain of soluble epoxide hydrolase. Biochem. Biophys. Res. Commun. 380, 188–192. https://doi.org/10.1016/j.bbrc.2009.01.079.
Caputi, L., Franke, J., Farrow, S.C., Chung, K., Payne, R.M.E., Nguyen, T.-D., Dang, T.-T.T., Soares Teto Carqueijeiro, I., Koudounas, K., Dugé de Bernonville, T., Ameyaw, B., Jones, D.M., Vieira, I.J.C., Courdavault, V., O'Connor, S.E., 2018. Missing enzymes in the biosynthesis of the anticancer drug vinblastine in Madagascar periwinkle. Science 360, 1235–1239. 80-. https://doi.org/10.1126/science.aat4100.
Cavill, G.W.K., Robertson, P.L., Brophy, J.J., Duke, R.K., McDonald, J., Plant, W.D., 1984. Chemical ecology of the meat ant, Iridomyrmex purpureus sens. strict. Insect Biochem. 14, 505–513. https://doi.org/10.1016/0020-1790(84)90004-0.
Chen, W., Viljoen, A.M., 2010. Geraniol - a review of a commercially important fragrance material. South Afr. J. Bot. 76, 643–651. https://doi.org/10.1016/j.sajb.2010.05.008.
Collu, G., Unver, N., Peltenburg-Looman, A.M.G., van der Heijden, R., Verpoorte, R., Memelink, J., 2001. Geraniol 10-hydroxylase, a cytochrome P450 enzyme involved in terpenoid indole alkaloid biosynthesis. FEBS Lett. 508, 215–220. https://doi.org/10.1016/s0014-5793(01)03045-9.
Dinda, B., 2019. Pharmacology of iridoids. In: Dinda, B. (Ed.), Pharmacology and Applications of Naturally Occurring Iridoids. Springer International Publishing, Cham 145–254. https://doi.org/10.1007/978-3-030-05575-2_5.
Frick, S., Nagel, R., Schmidt, A., Bodemann, R.R., Rahfeld, P., Pauls, G., Brandt, W., Gershenzon, J., Boland, W., Burse, A., 2013. Metal ions control product specificity of isoprenyl diphosphate synthases in the insect terpenoid pathway. Proc. Natl. Acad. Sci. 110, 4194–4199. https://doi.org/10.1073/pnas.1221489110.
Geu-Flores, F., Sherden, N.H., Courdavault, V., Burlat, V., Glenn, W.S., Wu, C., Nims, E., Cui, Y., O'Connor, S.E., 2012. An alternative route to cyclic terpenes by reductive cyclization in iridoid biosynthesis. Nature 492, 138–142. https://doi.org/10.1038/nature11692.
Ghisalberti, E.L., 1998. Biological and pharmacological activity of naturally occurring iridoids and secoiridoids. Phytomedicine 5, 147–163. https://doi.org/10.1016/S0944-7113(98)80012-3.
Greule, A., Stok, J.E., De Voss, J.J., Cryle, M.J., 2018. Unrivalled diversity: the many roles and reactions of bacterial cytochromes P450 in secondary metabolism. Nat. Prod. Rep. 35, 757–791. https://doi.org/10.1039/C7NP00063D.
Helvig, C., Koener, J.F., Unnithan, G.C., Feyereisen, R., 2004. CYP15A1, the cytochrome P450 that catalyzes epoxidation of methyl farnesoate to juvenile hormone III in cockroach corpora allata. Proc. Natl. Acad. Sci. 101, 4024–4029. https://doi.org/10.1073/pnas.0306980101.
Hofer, R., Boachon, B., Renault, H., Gavira, C., Miesch, L., Iglesias, J., Ginglinger, J.F., Allouche, L., Miesch, M., Grec, S., Larbat, R., Werck-Reichhart, D., 2014. Dual function of the cytochrome P450 CYP76 family from Arabidopsis thaliana in the metabolism of monoterpenols and phenylurea herbicides. Plant Physiol. 166, 1149–1161. https://doi.org/10.1104/pp.114.244814.
Hofer, R., Dong, L., Andre, F., Ginglinger, J.F., Lugan, R., Gavira, C., Grec, S., Lang, G., Memelink, J., Van der Krol, S., Bouwmeester, H., Werck-Reichhart, D., 2013. Geraniol hydroxylase and hydroxygeraniol oxidase activities of the CYP76 family of cytochrome P450 enzymes and potential for engineering the early steps of the (seco) iridoid pathway. Metab. Eng. 20, 221–232. https://doi.org/10.1016/j.ymben.2013.08.001.
Johnston, J.B., Ouellet, H., Podust, L.M., Ortiz de Montellano, P.R., 2011. Structural control of cytochrome P450-catalyzed ω-hydroxylation. Arch. Biochem. Biophys. 507, 86–94. https://doi.org/10.1016/j.abb.2010.08.011.
Joussen, N., Agnolet, S., Lorenz, S., Schone, S.E., Ellinger, R., Schneider, B., Heckel, D.G., 2012. Resistance of Australian Helicoverpa armigera to fenvalerate is due to the chimeric P450 enzyme CYP337B3. Proc. Natl. Acad. Sci. 109, 15206–15211. https://doi.org/10.1073/pnas.1202047109.
Keeling, C.I., Henderson, H., Li, M., Dullat, H.K., Ohnishi, T., Bohlmann, J., 2013. CYP345E2, an antenna-specific cytochrome P450 from the mountain pine beetle, Dendroctonus ponderosae Hopkins, catalyses the oxidation of pine host monoterpene volatiles. Insect Biochem. Mol. Biol. 43, 1142–1151. https://doi.org/10.1016/j.ibmb.2013.10.001.
Kellner, F., Geu-Flores, F., Sherden, N.H., Brown, S., Foureau, E., Courdavault, V., O'Connor, S.E., 2015. Discovery of a P450-catalyzed step in vindoline biosynthesis: a link between the aspidosperma and eburnamine alkaloids. Chem. Commun. 51, 7626–7628. https://doi.org/10.1039/C5CC01309G.
Krieger, E., Joo, K., Lee, Jinwoo, Lee, Jooyoung, Raman, S., Thompson, J., Tyka, M., Baker, D., Karplus, K., 2009. Improving physical realism, stereochemistry, and side-chain accuracy in homology modeling: four approaches that performed well in CASP8. Proteins Struct. Funct. Bioinforma. 77, 114–122. https://doi.org/10.1002/prot.22570.
Krieger, E., Vriend, G., 2014. YASARA View - molecular graphics for all devices - from smartphones to workstations. Bioinformatics 30, 2981–2982. https://doi.org/10.1093/bioinformatics/btu426.
Krithika, R., Srivastava, P.L., Rani, B., Kolet, S.P., Chopade, M., Soniya, M., Thulasiram, H.V., 2015. Characterization of 10-hydroxygeraniol dehydrogenase from Catharanthus roseus reveals cascaded enzymatic activity in iridoid biosynthesis. Sci. Rep. 5, 8258. https://doi.org/10.1038/srep08258.
Kunert, M., Rahfeld, P., Shaker, K.H., Schneider, B., David, A., Dettner, K., Pasteels, J.M., Boland, W., 2013. Beetles do it differently: two stereodivergent cyclisation modes in iridoid-producing leaf beetle larvae. Chembiochem 14, 353–360. https://doi.org/10.1002/cbic.201200689.
Kunert, M., Søe, A., Bartram, S., Discher, S., Tolzin-Banasch, K., Nie, L., David, A., Pasteels, J., Boland, W., 2008. De novo biosynthesis versus sequestration: a network of transport systems supports in iridoid producing leaf beetle larvae both modes of defense. Insect Biochem. Mol. Biol. 38, 895–904. https://doi.org/10.1016/j.ibmb.2008.06.005.
Larsen, B., Fuller, V.L., Pollier, J., Van Moerkercke, A., Schweizer, F., Payne, R., Colinas, M., O'Connor, S.E., Goossens, A., Halkier, B.A., 2017. Identification of iridoid glucoside transporters in Catharanthus roseus. Plant Cell Physiol. 58, 1507–1518. https://doi.org/10.1093/pcp/pcx097.
Laskowski, R.A., MacArthur, M.W., Moss, D.S., Thornton, J.M., 1993. PROCHECK: a program to check the stereochemical quality of protein structures. J. Appl. Crystallogr. 26, 283–291. https://doi.org/10.1107/S0021889892009944.
Laurent, P., Braekman, J.-C., Daloze, D., 2004. Insect chemical defense. In: Schulz, S. (Ed.), The Chemistry of Pheromones and Other Semiochemicals II. Springer Berlin Heidelberg, Berlin, Heidelberg, pp. 167–229. https://doi.org/10.1007/b98317.
Manikandan, P., Nagini, S., 2018. Cytochrome P450 structure, function and clinical significance: a review. Curr. Drug Targets 19, 38–54. https://doi.org/10.2174/1389450118666170125144557.
Miettinen, K., Dong, L., Navrot, N., Schneider, T., Burlat, V., Pollier, J., Woittiez, L., van der Krol, S., Lugan, R., Ilc, T., Verpoorte, R., Oksman-Caldentey, K.-M., Martinoia, E., Bouwmeester, H., Goossens, A., Memelink, J., Werck-Reichhart, D., 2014. The seco-iridoid pathway from Catharanthus roseus. Nat. Commun. 5, 3606. https://doi.org/10.1038/ncomms4606.
Nasiou, E., Giannakou, I.O., 2018. Effect of geraniol, a plant-based alcohol monoterpene oil, against Meloidogyne javanica. Eur. J. Plant Pathol. 152, 701–710. https://doi.org/10.1007/s10658-018-1512-x.
Nyati, P., Nouzova, M., Rivera-Perez, C., Clifton, M.E., Mayoral, J.G., Noriega, F.G., 2013. Farnesyl phosphatase, a corpora allata enzyme involved in juvenile hormone biosynthesis in Aedes aegypti. PLoS One 8, e71967. https://doi.org/10.1371/journal.pone.0071967.
Oldham, N.J., Veith, M., Boland, W., Dettner, K., 1996. Iridoid monoterpene biosynthesis in insects: evidence for a de novo pathway occurring in the defensive glands ofPhaedon armoraciae (chrysomelidae) leaf beetle larvae. Naturwissenschaften 83, 470–473. https://doi.org/10.1007/BF01144016.
Pasteels, J.M., Braekman, J.-C., Daloze, D., 1988. Chemical defense in the chrysomelidae. In: Jolivet, P., Petitpierre, E., Hsiao, T.H. (Eds.), Biology of Chrysomelidae, Series Entomologica. Springer Netherlands, Dordrecht, pp. 233–252. https://doi.org/10.1007/978-94-009-3105-3_14.
Qu, Y., Easson, M.L.A.E., Froese, J., Simionescu, R., Hudlicky, T., De Luca, V., 2015. Completion of the seven-step pathway from tabersonine to the anticancer drug precursor vindoline and its assembly in yeast. Proc. Natl. Acad. Sci. 112, 6224–6229. https://doi.org/10.1073/pnas.1501821112.
Rahfeld, P., Haeger, W., Kirsch, R., Pauls, G., Becker, T., Schulze, E., Wielsch, N., Wang, D., Groth, M., Brandt, W., Boland, W., Burse, A., 2015. Glandular β-glucosidases in juvenile Chrysomelina leaf beetles support the evolution of a host-plant-dependent chemical defense. Insect Biochem. Mol. Biol. 58, 28–38. https://doi.org/10.1016/j.ibmb.2015.01.003.
Rahfeld, P., Kirsch, R., Kugel, S., Wielsch, N., Stock, M., Groth, M., Boland, W., Burse, A., 2014. Independently recruited oxidases from the glucose-methanol-choline oxidoreductase family enabled chemical defences in leaf beetle larvae (subtribe Chrysomelina) to evolve. Proc. R. Soc. Biol. Sci. 281, 20140842. https://doi.org/10.1098/rspb.2014.0842.
Raspotnig, G., Kaiser, R., Stabentheiner, E., Leis, H.-J., 2008. Chrysomelidial in the opisthonotal glands of the oribatid mite, Oribotritia berlesei. J. Chem. Ecol. 34, 1081–1088. https://doi.org/10.1007/s10886-008-9508-1.
Sadd, B.M., Barribeau, S.M., Bloch, G., de Graaf, D.C., Dearden, P., Elsik, C.G., Gadau, J., Grimmelikhuijzen, C.J.P., Hasselmann, M., Lozier, J.D., Robertson, H.M., Smagghe, G., Stolle, E., Van Vaerenbergh, M., Waterhouse, R.M., Bornberg-Bauer, E., Klasberg, S., Bennett, A.K., Câmara, F., Guigó, R., Hoff, K., Mariotti, M., Munoz-Torres, M., Murphy, T., Santesmasses, D., Amdam, G.V., Beckers, M., Beye, M., Biewer, M., Bitondi, M.M.G., Blaxter, M.L., Bourke, A.F.G., Brown, M.J.F., Buechel, S.D., Cameron, R., Cappelle, K., Carolan, J.C., Christiaens, O., Ciborowski, K.L., Clarke, D.F., Colgan, T.J., Collins, D.H., Cridge, A.G., Dalmay, T., Dreier, S., du Plessis, L., Duncan, E., Erler, S., Evans, J., Falcon, T., Flores, K., Freitas, F.C.P., Fuchikawa, T., Gempe, T., Hartfelder, K., Hauser, F., Helbing, S., Humann, F.C., Irvine, F., Jermiin, L.S., Johnson, C.E., Johnson, R.M., Jones, A.K., Kadowaki, T., Kidner, J.H., Koch, V., Köhler, A., Kraus, F.B., Lattorff, H.M.G., Leask, M., Lockett, G.A., Mallon, E.B., Antonio, D.S.M., Marxer, M., Meeus, I., Moritz, R.F.A., Nair, A., Näpflin, K., Nissen, I., Niu, J., Nunes, F.M.F., Oakeshott, J.G., Osborne, A., Otte, M., Pinheiro, D.G., Rossié, N., Rueppell, O., Santos, C.G., Schmid-Hempel, R., Schmitt, B.D., Schulte, C., Simões, Z.L.P., Soares, M.P.M., Swevers, L., Winnebeck, E.C., Wolschin, F., Yu, N., Zdobnov, E.M., Aqrawi, P.K., Blankenburg, K.P., Coyle, M., Francisco, L., Hernandez, A.G., Holder, M., Hudson, M.E., Jackson, L., Jayaseelan, J., Joshi, V., Kovar, C., Lee, S.L., Mata, R., Mathew, T., Newsham, I.F., Ngo, R., Okwuonu, G., Pham, C., Pu, L.-L., Saada, N., Santibanez, J., Simmons, D., Thornton, R., Venkat, A., Walden, K.K.O., Wu, Y.-Q., Debyser, G., Devreese, B., Asher, C., Blommaert, J., Chipman, A.D., Chittka, L., Fouks, B., Liu, J., O'Neill, M.P., Sumner, S., Puiu, D., Qu, J., Salzberg, S.L., Scherer, S.E., Muzny, D.M., Richards, S., Robinson, G.E., Gibbs, R.A., Schmid-Hempel, P., Worley, K.C., 2015. The genomes of two key bumblebee species with primitive eusocial organization. Genome Biol. 16, 76. https://doi.org/10.1186/s13059-015-0623-3.
Sandstrom, P., Ginzel, M.D., Bearfield, J.C., Welch, W.H., Blomquist, G.J., Tittiger, C., 2008. Myrcene hydroxylases do not determine enantiomeric composition of pheromonal ipsdienol in Ips spp. J. Chem. Ecol. 34, 1584–1592. https://doi.org/10.1007/s10886-008-9563-7.
Sandstrom, P., Welch, W.H., Blomquist, G.J., Tittiger, C., 2006. Functional expression of a bark beetle cytochrome P450 that hydroxylates myrcene to ipsdienol. Insect Biochem. Mol. Biol. 36, 835–845. https://doi.org/10.1016/j.ibmb.2006.08.004.
Sevrioukova, I.F., 2017. High-level production and properties of the cysteine-depleted cytochrome P450 3A4. Biochemistry 56, 3058–3067. https://doi.org/10.1021/acs.biochem.7b00334.

Sezutsu, H., Le Goff, G., Feyereisen, R., 2013. Origins of P450 diversity. Philos. Trans. R. Soc. Lond. B Biol. Sci. 368, 20120428. https://doi.org/10.1098/rstb.2012.0428.

Sippl, M.J., 1993. Recognition of errors in three-dimensional structures of proteins. Proteins Struct. Funct. Genet. 17, 355–362. https://doi.org/10.1002/prot.340170404.

Sippl, M.J., 1990. Calculation of conformational ensembles from potentials of mena force. J. Mol. Biol. 213, 859–883. https://doi.org/10.1016/S0022-2836(05)80269-4.

Smith, R.M., Brophy, J.J., Cavill, G.W.K., Davies, N.W., 1979. Iridodials and nepetalactone in the defensive secretion of the coconut stick insects,Graeffea crouani. J. Chem. Ecol. 5, 727–735. https://doi.org/10.1007/BF00986557.

Snyder, J.H., Qi, X., 2013. Biosynthesis: metal matters. Nat. Chem. Biol. 9, 295–296. https://doi.org/10.1038/nchembio.1232.

Song, M., Kim, A.C., Gorzalski, A.J., MacLean, M., Young, S., Ginzel, M.D., Blomquist, G.J., Tittiger, C., 2013. Functional characterization of myrcene hydroxylases from two geographically distinct Ips pini populations. Insect Biochem. Mol. Biol. 43, 336–343. https://doi.org/10.1016/j.ibmb.2013.01.003.

Stock, M., Gretscher, R.R., Groth, M., Eiserloh, S., Boland, W., Burse, A., 2013. Putative sugar transporters of the mustard leaf beetle Phaedon cochleariae: their phylogeny and role for nutrient supply in larval defensive glands. PLoS One 8, e84461. https://doi.org/10.1371/journal.pone.0084461.

Strauss, A.S., Peters, S., Boland, W., Burse, A., 2013. ABC transporter functions as a pacemaker for sequestration of plant glucosides in leaf beetles. Elife 2, e01096. https://doi.org/10.7554/eLife.01096.

Sung, P.-H., Huang, F.-C., Do, Y.-Y., Huang, P.-L., 2011. Functional expression of geraniol 10-Hydroxylase reveals tts dual function in the biosynthesis of terpenoid and phenylpropanoid. J. Agric. Food Chem. 59, 4637–4643. https://doi.org/10.1021/jf200259n.

Sutherland, T.D., Unnithan, G.C., Andersen, J.F., Evans, P.H., Murataliev, M.B., Szabo, L.Z., Mash, E.A., Bowers, W.S., Feyereisen, R., 1998. A cytochrome P450 terpenoid hydroxylase linked to the suppression of insect juvenile hormone synthesis. Proc. Natl. Acad. Sci. 95, 12884–12889. https://doi.org/10.1073/pnas.95.22.12884.

Tundis, R., Loizzo, M., Menichini, Federica, Statti, G., Menichini, Francesco, 2008. Biological and pharmacological activities of iridoids: recent developments. Mini Rev. Med. Chem. 8, 399–420. https://doi.org/10.2174/138955708783955926.

Veith, M., Lorenz, M., Boland, W., Simon, H., Dettner, K., 1994. Biosynthesis of iridoid monoterpenes in insects: defensive secretions from larvae of leaf beetles (coleoptera: chrysomelidae). Tetrahedron 50, 6859–6874. https://doi.org/10.1016/S0040-4020(01)81338-7.

Yamane, H., Konno, K., Sabelis, M., Takabayashi, J., Sassa, T., Oikawa, H., 2010. Chemical defence and toxins of plants. In: Comprehensive Natural Products II. Elsevier, Oxford, pp. 339–385. https://doi.org/10.1016/B978-008045382-8.00099-X.

Yang, T., Liu, N., 2011. Genome analysis of cytochrome P450s and their expression profiles in insecticide resistant mosquitoes, Culex quinquefasciatus. PLoS One 6, e29418. https://doi.org/10.1371/journal.pone.0029418.